IUST Iran University of Science and Technology

Iranian Journal of Electrical and Electronic Engineering

Journal Homepage: ijeee.iust.ac.ir

An Improved Control Approach for Dual Mechanical Coupled BLDC Motor With Nine-Switch Inverter

M. Sanatgar*, M. R. Alizadeh Pahlavani*(C.A.) and A. Bali Lashak*

Abstract: This paper presents the control approach for single inverter dual coupled brushless DC motors (DCBLDC) drive system. One of the basic requirements of such systems, is the power balance between two motors and on the other hand, minimizing mechanical fluctuations in order to avoid mechanical equipment damage especially in the state of mechanical resonance. This paper also presents an improved form of the conventional direct torque control (IDTC) for the DCBLDC, which can be used on nine-switch inverters (NSIs). The conventional approaches used in the coupled motors are considered, and then a combination of torque and velocity control is proposed for DCBLDC. After theoretical analysis and drive modeling, whose performance has been simulated by MATLAB/Simulink in terms of dispatching balanced power as well as dealing with transient phenomena owing to malfunctioning of the mechanical connection line. Finally, experiments with the 120W BLDC motors are executed to verify the feasibility of the proposed approach.

Keywords: Coupled Motors, Double Drive, DTC, Load Balance Distribution, Nine-Switch Inverter.

1 Nomenclature

S_{QU}, S_{QM}, S_{QL}	Upper, middle and lower switches of NSI.
J_{m1}, J_{m2}	BLDCs inertia.
J_{p1}, J_{p2}, J_{p3}	Pulleys inertia.
J_L	Load total inertia.
θ_{p1}, θ_{p1}, θ_{p3}	Pulleys positions.
K_{D1}, K_{D2}, K_{D3}	Pulleys gear tooth damping coefficients.
K_{S1}, K_{S2}, K_{S3}	Pulleys gear tooth stiffness coefficients.
T_{e1}, T_{e2}	Motors electromagnetic torque.
T_L	Load torque.
P_1, P_2	Motors Instantaneous power.
k_b, k_t	BEMF, Torque coefficients.
i_α, i_β	Alpha- and beta- axis currents.
V_α, V_β	Alpha- and beta- axis voltages.
φ_α, φ_β	Alpha- and beta- axis fluxes.
R, L, M	Stator resistance, self and mutual inductance.
CK	Clarke transformation.
P_{N1}, P_{N2}	Motors rated power.
V_s, e_s	Stator voltage, BEMF

Iranian Journal of Electrical and Electronic Engineering, 2019.
Paper first received 09 May 2018 and accepted 26 January 2019.
* The authors are with the Malek-Ashtar University of Technology, Lavizan, Tehran, Iran.
E-mails: m.sanatgar1985@gmail.com, mr_alizadehp@mut.ac.ir and arefbali@ymail.com.
Corresponding Author: M. R. Alizadeh Pahlavani.

1 Introduction

SINCE the advances in power switching devices, such as IGBTs and MOSFETs, the prices of power switching devices have continually decreased. Such improvements have led to enhancing features such as current rating and break down voltage, voltage drop and switching losses of these devices [1]. Nevertheless, these elements are still one of the most costly parts of an energy conversion system. Therefore, in recent years, many efforts have been made to reduce the energy conversion system costs. Especially, for the fields where the cost is critically concerned such as home appliances and small machine drive application.

Eliminating the position or velocity sensors [2-6], current sensing methods using resistors [7-10], and setting up parallel dual/multi machines drives [11-14]

are the representative efforts for the hardware reduction. Among all these works, parallel machines drive technique is less attractive for researchers and manufacturers due to problems in the synchronized velocity operation and inappropriate system performance compared to other techniques. However, the parallel motor drive technique for the applications where the synchronized velocity operation is endurable such as fans, pumps, electric traction, multi drive conveyors and railroads is very efficient. In addition, in the parallel machines drive technique, the duplicated components of the system, including the input filter, rectifier, controller, inverter, protection circuit, and other communication devices, will be eliminated leading to lower costs and system dimensions. Many studies have been carried out for setting up of single inverter dual parallel (SIDP) motor drive system [11, 15]. Despite the presentation of various control methods in SIDPs, due to its inherent instability risk, few control methods have been reported for the SIDP drive system. Regarding the widespread use of PMSMs due to its high power density and high efficiency, studies about the SIDP PMSM drive are reported in [16]. In [17] and [18], the multi PMSMs drive system analyses, along with its control approach based on higher torque machine were presented. In [18], the predictive control method is provided for SIDP of PMSMs. The average current control method is given in [19], and the control method which controls both average and differential currents are given in [20]. Although the above works have been succeeded to drive parallel PMSMs using a single inverter, but, in all of these activities, mechanical damping or model-based control are used to maintain system stability, which makes it difficult to be used in a variety of applications. The maximum torque per ampere method (MTPA) for SIDP of PMSMs is also studied in [20]. Although MTPA method has proposed some solutions but it is not operational due to the numerous calculation burdens. In many drive systems with two motors, a single inverter with common output is used to feed two motors, so that both motors run at the same frequencies and voltages. Ideally, and assuming that motors with the same rated power and common characteristics are selected, using a common velocity controller for two motors will result in the generation of equal electromagnetic torques and, consequently, equal power transmission between the motors. While, in practice due to differences in the manufacture and production of motors and electronic components, fluctuation and even instability will be imposed to the system. In addition, issues of uncertainty in system modeling, measurement noise, and external disturbances of the system are among the factors that underlie using a single inverter with common output for controlling two motors and achieving desire electromagnetic torque and velocities.

In this paper, using a compact NSI and a single control board, two coupled BLDC motors are independently driven and controlled. The connection of the motors to each other and to the load is implemented via the connection belt. Therefore, the belt demolition of the connection is modeled as a disturbance of system and its effects on the drive system are evaluated as well. Different control approaches, including velocity control and torque control, are compared with each other, and finally, to overcome the drawbacks of the aforementioned approaches a combination of torque and velocity controller is recommended as the most appropriate approach to control the DCBLDC. The control method used for this system is an improved form of the conventional DTC that can be used on NSIs. The accuracy of its performance in terms of power balance and the counteraction of transient phenomena caused by external disturbances have been well verified.

2 Dynamic Behavior Model of Two BLDC Coupled Motors

Nowadays, use of two motors in the place of a single motor having complicated structure has found wide application in industries. Parallel or series operating electrical motors with independent mechanical load are very common. Building permanent magnet (PM) motors with the rating above 120 kW is difficult because of the PM limitation, therefore two 120 kW motors have been used instead of a single 240 kW PM synchronous motor in a fuel–cell system [21]. In this case, two identical motors operate in parallel with no dynamic coupling which facilitates the load sharing. Two switched reluctance motors in a locomotive [22, 23], two brushless AC motors in a ship [24] and two DC motors as buoyant wings with fish-like behavior [25], are examples of parallel operating electrical motors.

The electromechanical system studied in this paper is illustrated in Fig. 1(a), which is composed using two independent sub-systems, each one consist of one motor, a pulley, and a common belt. Two BLDC motors as system drivers, a brushed DC motor as a load, and three pulleys attached to the shaft of each motor as well as connection belt between them as a power transmission system from drivers to the loads have been considered. It is worth noting that, for large power, belt and pulley are substituted by gears. First, a sketch map of the mechanical connection line has been made, and a mathematical electromechanical model has been simulated using the MATLAB/Simulink. The motors shaft have been supposed as rigid while the pulley tooth have been supposed as flexible, and so damping and stiffness coefficients of the pulleys have been used at the theoretical model. According to the mechanical transfer system that is included two pulleys coupled with a common belt (Fig. 1), the probability of a mechanical load imbalance between two motors due to the difference in pulleys stiffness [26] and the slip between the belt and the pulleys [27], the angular velocity differences at the inlet and outlet of the motor

shaft will be expected due to the belt tension and strain [28-30]. According to the dynamic model presented in Fig. 1(b), the following relationships can be calculated.

$$(J_{m1}+J_{p1})\ddot{\theta}_{p1}=T_{e1}-K_{D1}(\dot{\theta}_{p1}-\dot{\theta}_{p3})-K_{S1}(\theta_{p1}-\theta_{p3}) +K_{D3}(\dot{\theta}_{p1}-\dot{\theta}_{p2})+K_{S3}(\theta_{p1}-\theta_{p2}) \quad (1)$$

$$(J_{m2}+J_{p2})\ddot{\theta}_{p2}=T_{e2}+K_{D2}(\dot{\theta}_{p2}-\dot{\theta}_{p3})+K_{S2}(\theta_{p2}-\theta_{p3}) -K_{D3}(\dot{\theta}_{p2}-\dot{\theta}_{p1})-K_{S3}(\theta_{p2}-\theta_{p1}) \quad (2)$$

$$(J_L+J_{p3})\ddot{\theta}_{p3}+K_{D1}(\dot{\theta}_{p3}-\dot{\theta}_{p1})+K_{S1}(\theta_{p3}-\theta_{p1}) +K_{D2}(\dot{\theta}_{p3}-\dot{\theta}_{p2})+K_{S2}(\theta_{p3}-\theta_{p2})=T_L \quad (3)$$

The symbols are defined in the nomenclature. The parameters used in Eqs. (1)-(3) are given in Table 1.

3 Nine-Switch Inverter

A nine-switch converter is consists of three switches in each arm and two input or output terminals in accordance with Fig. 2. The nine-switch converter has 33% and 50% of switch numbers in comparison with the back-to-back and the matrix converter, respectively [31, 32]. Based on output terminals frequency, two approaches are proposed for NSI modulation that is investigated by the authors in [33], for simulate the drive's electrical system, two 120 W 3-phase 4-poles brushless motors supplied by a NSI and MOSFET switches have been used.

4 BLDC Motors Modelling Units

In the modeling of BLDC motor, the effect of windings damping, salient rotor and rotor induction current have been neglected due to the stator harmonic field, iron and eddy losses, and the magnetic saturation effect. It is assumed that the stator windings are symmetrical. For this system, the index 1 and 2 in each term refers to its association with the motor connected to the inverter up or bottom terminal respectively. For example, i_{as1} represents the current corresponding to phase A across the motor connected to the upper terminal. The motor electrical properties can be modeled as (4)-(6) [34].

$$\begin{bmatrix} V_{as1}-e_{as1}\\ V_{bs1}-e_{bs1}\\ V_{cs1}-e_{cs1}\\ V_{as2}-e_{as2}\\ V_{bs2}-e_{bs2}\\ V_{cs2}-e_{cs2}\end{bmatrix}=\begin{bmatrix} R_1&0&0&0&0&0\\ 0&R_1&0&0&0&0\\ 0&0&R_1&0&0&0\\ 0&0&0&R_2&0&0\\ 0&0&0&0&R_2&0\\ 0&0&0&0&0&R_2\end{bmatrix}\begin{bmatrix} i_{as1}\\ i_{bs1}\\ i_{cs1}\\ i_{as2}\\ i_{bs2}\\ i_{cs2}\end{bmatrix}+\begin{bmatrix} L_1-M_1&0&0&0&0&0\\ 0&L_1-M_1&0&0&0&0\\ 0&0&L_1-M_1&0&0&0\\ 0&0&0&L_2-M_2&0&0\\ 0&0&0&0&L_2-M_2&0\\ 0&0&0&0&0&L_2-M_2\end{bmatrix}\frac{d}{dt}\begin{bmatrix} i_{as1}\\ i_{bs1}\\ i_{cs1}\\ i_{as2}\\ i_{bs2}\\ i_{cs2}\end{bmatrix} \quad (4)$$

$$\begin{bmatrix} e_{as1}\\ e_{bs1}\\ e_{cs1}\end{bmatrix}=\frac{k_{b1}}{2}\begin{bmatrix} e_1(\theta_1)\\ e_1(\theta_1-2\pi/3)\\ e_1(\theta_1+2\pi/3)\end{bmatrix}\omega_1,\quad \begin{bmatrix} e_{as2}\\ e_{bs2}\\ e_{cs2}\end{bmatrix}=\frac{k_{b2}}{2}\begin{bmatrix} e_2(\theta_2)\\ e_2(\theta_2-2\pi/3)\\ e_2(\theta_2+2\pi/3)\end{bmatrix}\omega_2 \quad (5)$$

$$e_2(\theta_2)=\begin{cases} 1 & 0\le\theta_2\le 2\pi/3\\ 1-\frac{6}{\pi}(\theta_2-\frac{2\pi}{3}) & 2\pi/3\le\theta_2\le\pi\\ -1 & \pi\le\theta_2\le 5\pi/3\\ -1+\frac{6}{\pi}(\theta_2-\frac{5\pi}{3}) & 5\pi/3\le\theta_2\le 2\pi\end{cases},\quad e_1(\theta_1)=\begin{cases} 1 & 0\le\theta_1\le 2\pi/3\\ 1-\frac{6}{\pi}(\theta_1-\frac{2\pi}{3}) & 2\pi/3\le\theta_1\le\pi\\ -1 & \pi\le\theta_1\le 5\pi/3\\ -1+\frac{6}{\pi}(\theta_1-\frac{5\pi}{3}) & 5\pi/3\le\theta_1\le 2\pi\end{cases} \quad (6)$$

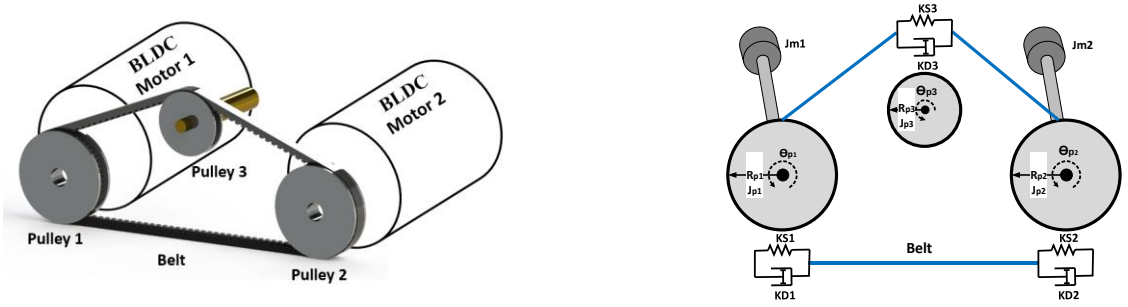

(a) (b)

Fig. 1 Dual BLDC motor drive: a) topology of a DCBLDC drive and b) mechanical connection model of DCBLDC.

Table 1 Characteristics-values of the mechanical connection line.

Motors	J_{m1}, J_{m2}	6.2e-4 [kg.m^2]
Pulleys	J_{p1}, J_{p2}	2e-5 [kg.m^2]
Pulley Stiffness	K_{D1}, K_{D2}, K_{D3}	20 [N.m.s/rad]
	K_{S1}, K_{S2}, K_{S3}	10e3 [N.m/rad]
Load	T_L	0.5 [N.m]

The electromagnetic torque of each of the motors is:

$$T_{e1}=\frac{k_{t1}}{2}\left(e_1(\theta_1)i_{as1}+e_1(\theta_1-\frac{2\pi}{3})i_{bs1}+e_1(\theta_1+\frac{2\pi}{3})i_{cs1}\right)$$
$$T_{e2}=\frac{k_{t2}}{2}\left(e_2(\theta_2)i_{as2}+e_2(\theta_2-\frac{2\pi}{3})i_{bs2}+e_2(\theta_2+\frac{2\pi}{3})i_{cs2}\right) \quad (7)$$

5 Improved Control Method

Given the great advantages of direct torque control (DTC) [35], such as high starting torque and fast dynamic response in transient conditions, this method is chosen as the best option for setting up and controlling the DCBLDC.DTC uses the motor modeling in the alpha-beta stationary frame and the following relationships. The DTC method proposed for the NSI is illustrated in Fig. 3. In this method, two conventional DTC modules with a two-phase conduction mode are used to generate nine-switched inverter switching pulses. Each DTC module has independent reference signals that can be used to control the up and down terminal voltages. The DTC equation of each of the motors is:

$$\begin{bmatrix}\vec{V}_\alpha\\ \vec{V}_\beta\end{bmatrix}=[CK]\begin{bmatrix}\vec{V}_a\\ \vec{V}_b\\ \vec{V}c\end{bmatrix},\ \begin{bmatrix}\vec{I}_\alpha\\ \vec{I}_\beta\end{bmatrix}=[CK]\begin{bmatrix}\vec{I}_a\\ \vec{I}_b\\ \vec{I}c\end{bmatrix} \quad (8)$$

$$\vec{\psi}_\alpha=\int(\vec{V}_\alpha-\vec{I}_\alpha R_s)dt,\ \ \vec{\psi}_\beta=\int(\vec{V}_\beta-\vec{I}_\beta R_s)dt \quad (9)$$

$$T=p(\psi_\alpha I_\beta-\psi_\beta I_\alpha),\ \mathrm{CK}=\sqrt{\frac{2}{3}}\begin{bmatrix}1 & -1/2 & -1/2\\ 0 & -\sqrt{3}/2 & \sqrt{3}/2\end{bmatrix} \quad (10)$$

Twelve outputs from switching pulses generated by two DTC modules are used to apply the NSI. So that, the middle-switching pulses in the NSI are derived from the logical XOR of the down-switches in up module with up-switches in down module.

The major problems that must be eliminated by the controller are as follows:

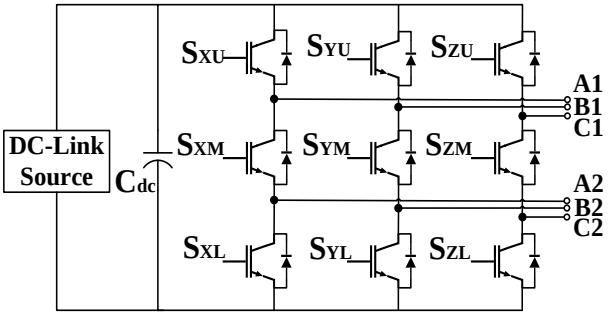

Fig. 2 NSI topology [31, 33].

1) Unbalanced load sharing between the two motors results in undesirable over-load on the motors and reduction of the efficiency of the other motor due to load reduction.
2) It is possible that one of the motors operates as generator mode, therefore, the controller must be designed in such a way that the load is distributed based on motors rated power as follows:

$$\frac{P_1}{P_2}=\frac{P_{N1}}{P_{N2}} \quad (11)$$

As (11), the load is distributed in terms of the rated power of the two motors. On the other hand, a higher-rated motor handles more load than the other one.

6 Dual Motor Drives (DMDs)

As previously described, this system is accomplished using single inverter with two separate outputs to feed the DMDs in order to access acceptable accessibility and to reduce the contingencies of an unplanned shutdown. As regards to the need for an adjusted velocity set point, the one of two motors must needfully influence the velocity, and hence it should be controlled by a velocity controller whereas the second motor can be torque or velocity controlled. Regarding the mechanical connection line consisting of three pulleys couplings with a common elastic belt, (Fig. 1), the probability of a mechanical load imbalance between two motors due to the

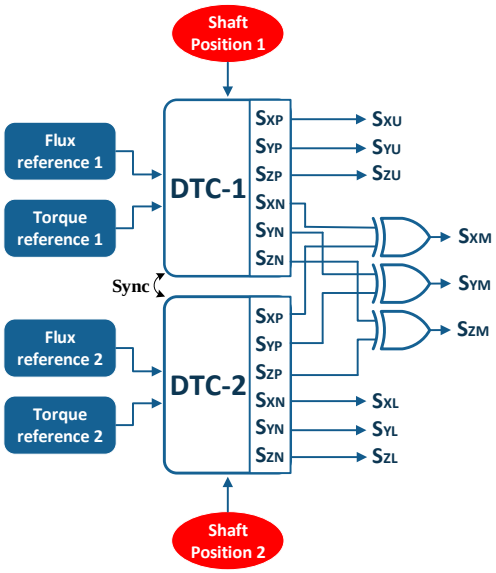

Fig. 3 Improved form of the DTC for the NSI.

difference in pulleys stiffness coefficients [26] and the slip between the belt and the pulleys [27], the angular velocity differences at the inlet and outlet of the motor shaft will be expected due to the belt tension and strain [28-30]. DMD operation in a leader–helper control method and both motors with the similar velocity reference is shown in Fig. 4(a). The point *A* relates to the leader drive (M1) and the *Á* to the desired operation point of the helper (M2) in order to make a balanced load sharing. Because of the independent voltages produced by the inverters, the second electromagnetic torque is maybe to fluctuate between *B* and *C* at the state of a momentary variation of the motors load. For the state of torque-controlled in helper motor, the motor velocity fluctuates between points *D* and *E* (Fig. 4(b)).

Generally, in a dual coupled motors, in order to specify the load velocity, the one motor should be controlled by a velocity controller, while the second motor can be controlled by either torque or velocity controller. In an ideal connection line, both torque and velocity controls ensure an identical load sharing. However, a slight angular displacement between the two motors, which is maybe to exist because of wear and tear in the connection belt or due to variation pulleys stiffness coefficient or even because of a tooth wear, be serious likely. The system operation in a unexpected variation of the stiffness coefficient at the second pulley tooth k_{p2} is investigated making apply of a velocity controller at the leader motor (M1) and studding separately the utilization of a torque or velocity controller at the helper one (M2). Such a mechanical breakdown may appear in the state of exhaustion from continuous work or manufacturing problems. In this paper, the performance of the DCBLDC having a steady variation at the connection line is also studied having the leader velocity controlled and considering to the used control approach of the helper. This steady variation is simulated using different the stiffness coefficient at the second pulley (k_{p2} = 0.6 k_{p1}).

6.1 Leader Velocity Controlled–Helper Velocity Controlled

In this approach, both motors control by velocity controller having the similar velocity reference. A diagram of this approach is figured in Fig. 5. In this method, the motor real velocities are compared with the desired velocity, and also the velocity error is applied to a PI controller that generates a torque set point used by the IDTC algorithm. In this approach, the motors are worked separately. The motors run from 0 to 200 r/min in t = 10 ms following a corresponding velocity reference. The velocity reference remains at 200 r/min until t = 150 ms. An unexpected variation of the stiffness coefficient at the second pulley tooth to the 60% of its previous value is simulated at t = 150 ms. The motor torques and also the motor velocities simulation results are shown in Fig. 6. Configuring the two separate PI-velocity controllers, the proportional-gain and the integral-gain was adjust to k_p = 1 and k_i = 50, respectively. By using the two separate velocity controller for both motors, the motor velocities stay near to the velocity reference of 200 r/min similar before the variation of the stiffness coefficient at the second

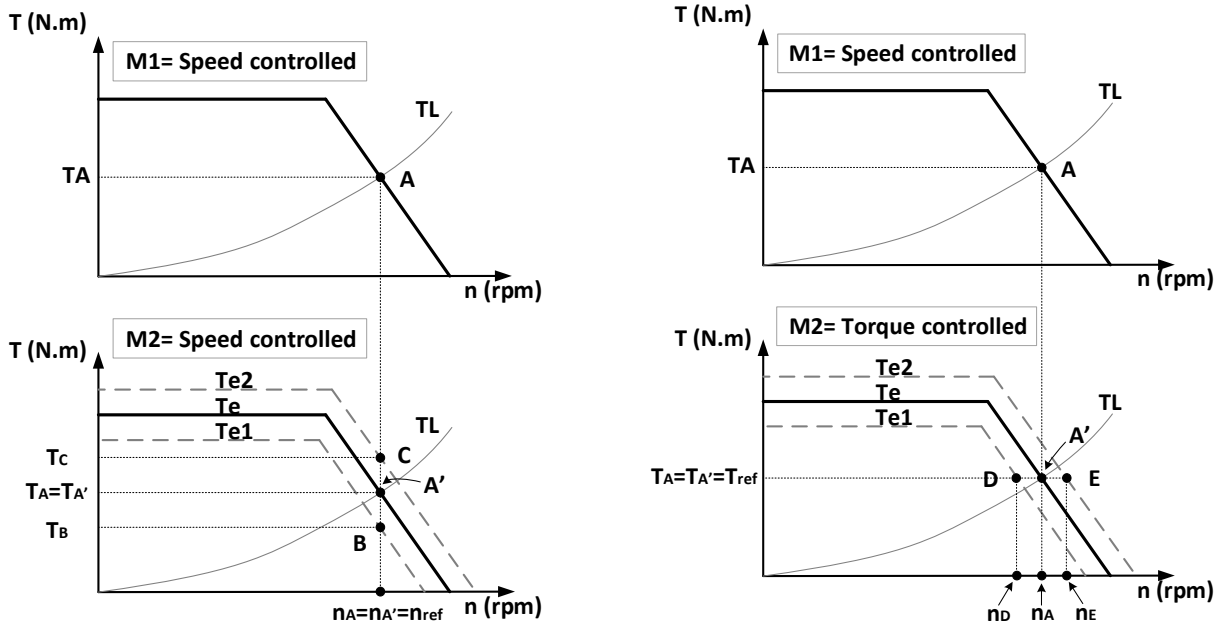

(a) (b)

Fig. 4 Dual BLDC motor drive: a) topology of a DCBLDC drive and b) mechanical connection model of DCBLDC. Leader–helper control method—motors fed from independent inverters. a) leader (M1) and helper (M2) motors at velocity control and b) velocity controlled at leader motor (M1) and torque controlled at helper motor (M2).

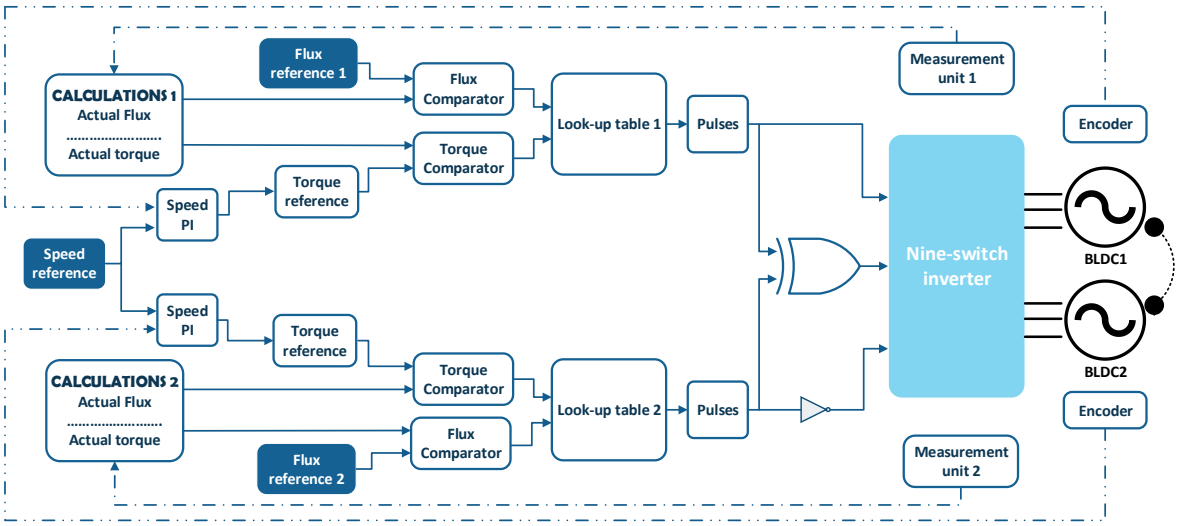

Fig. 5 Diagram of the control approach of DCBLDC operation: both leader (M1) and helper (M2) are velocity controlled.

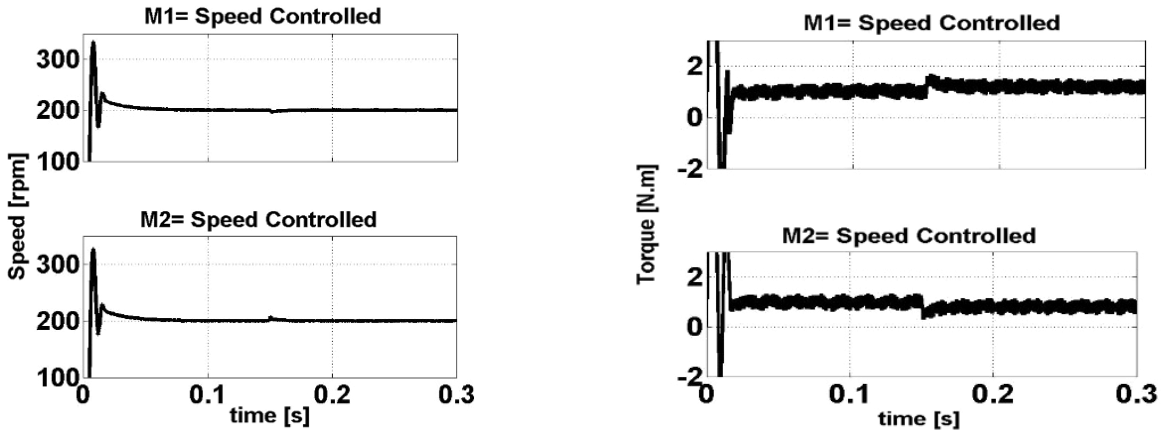

(a) (b)

Fig. 6 Velocity controller at both leader and helper motors with a 40% reduction of the helper pulleys stiffness coefficient k_{p2} at t = 150 ms.

pulley. Contrarily, before the advent of the mechanical abnormality, the motor torques are the same, there is a major overloading of the first motor after t = 150 ms. In this situation, due to the appearance of the sudden variation of the mechanical connection line, the applied load on the first motor is upper than the second one and the dual separated velocity control force the motors to maintain their velocity stable, the first motor carries more percentage of the whole load. It has also been mentioned previously at Fig. 4(a). For 10 < t < 150 ms in the steady-state, the two BLDC motors work at point *A* and *Á*, respectively, having identical velocity and also the same torque. Due to the load variation at t = 150 ms together with the dual separated velocity controller, the real second motor operation point will move to *B*. Simultaneously, the first operation point will be gone to another position having same velocity and generating a higher torque leading to an unbalanced load sharing.

In the state of a steady exhaustion at the connection line, the mechanical burden on the first motor is higher. In order to simulate this situation, the stiffness coefficient at the second pulley tooth was investigated to be steadily equal to 60% of its previous value. In Fig. 7 can be obviously considered that at the start-up time as well as on a steady-state duration, the first motor torque is upper than the second one. This means that although the real velocities of two motors are quite the same, the first motor caries upper value of the total mechanical load, so the total required power is not symmetrically shared between two BLDC motors.

6.2 Leader Velocity Controlled–Helper Torque Controlled

According to Fig. 8 In this approach, the first motor is controlled by velocity and the second by torque controller, that means the leader PI-velocity controller generates a torque set point for the helper motor. Thus, the torque set point could be transferred from the leader to the helper, in the specific NSI configuration with one control board do not requires the two inverters to be able to intercommunicate to each other. Like to part A, a unexpected decrease of the stiffness coefficient at the

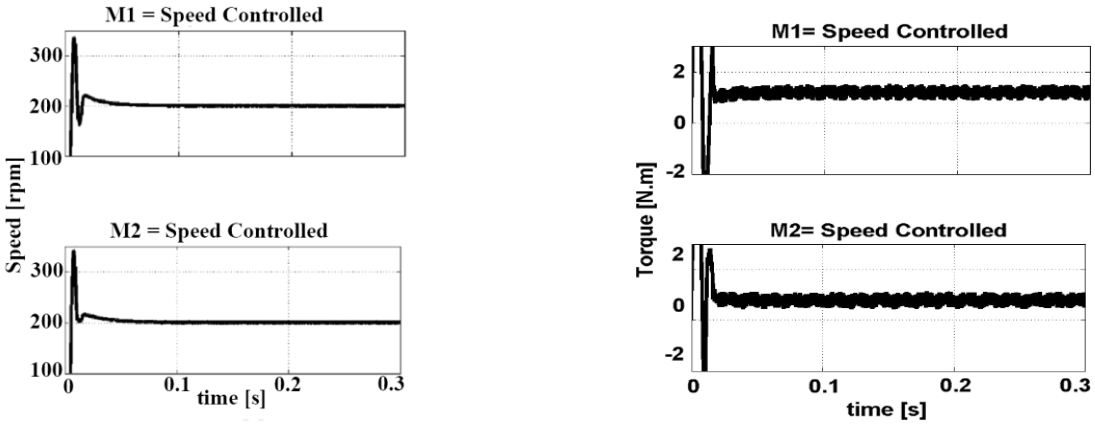

(a) (b)

Fig. 7 Velocity controller at both leader and helper motors with a steady variation at the pulley stiffness coefficients ($k_{p2} = 0.6k_{p1}$).

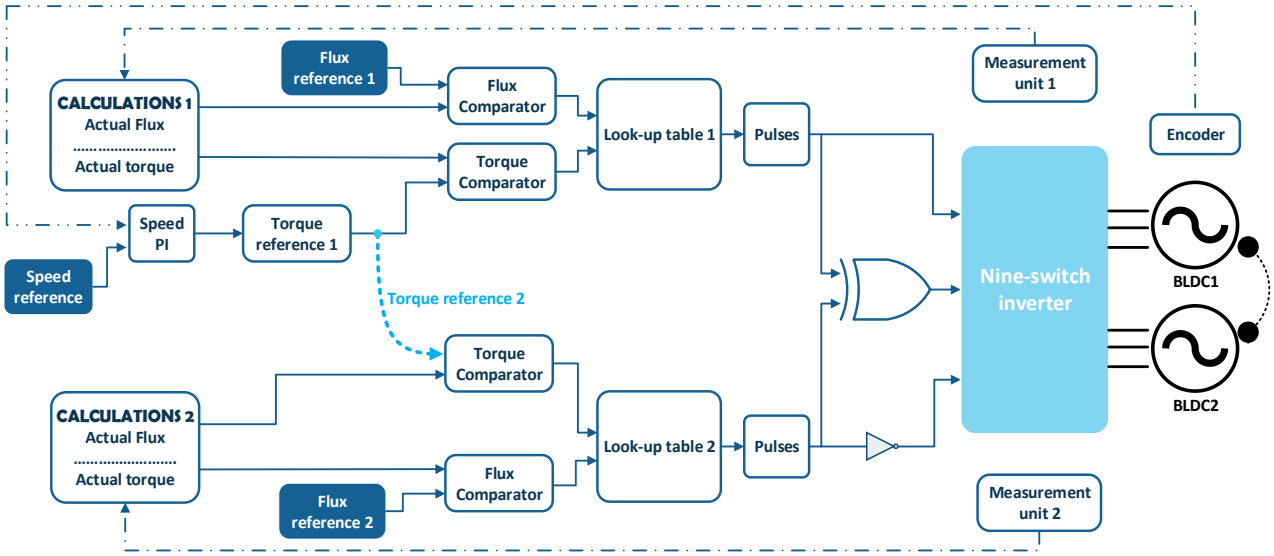

Fig. 8 Diagram of the control approach of DCBLDC operation: Leader motor (M1) is velocity controlled, and helper motor (M2) is torque controlled.

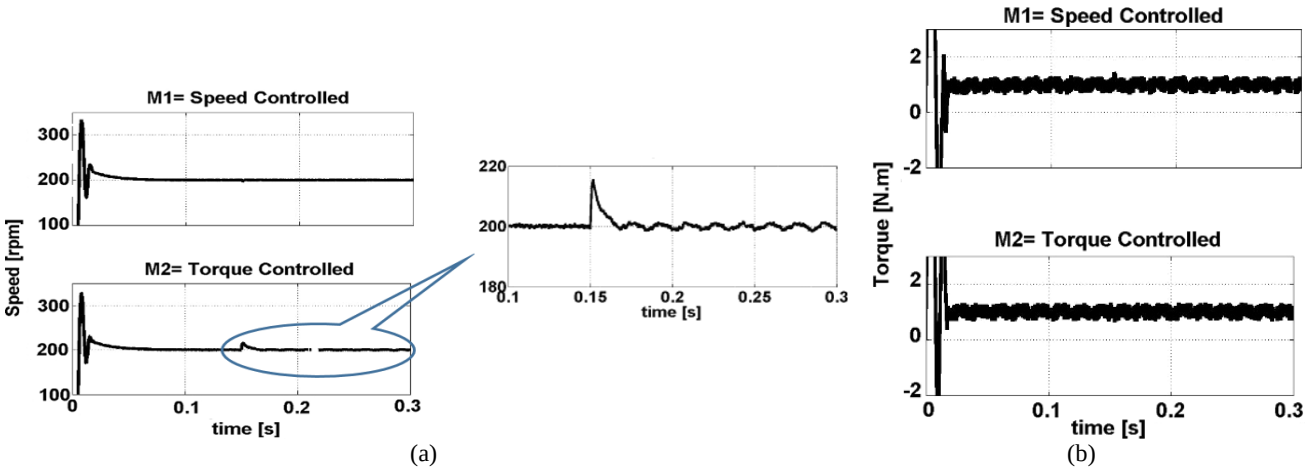

(a) (b)

Fig. 9 Leader–helper motor performance applying a velocity controller at the leader motor and a torque controller at the helper: with 40% reduction of the helper pulley stiffness coefficient k_{p2} at $t = 15$ s.

second pulley coupling to the 60% of its previous value has been considered, and also the results of this decrease at the both motor torques and the motor velocities are illustrated in Fig. 9 remaining the same configuration for the Leader PI-velocity controller (k_p = 1, k_i = 50).

After the sudden variation of the pulley stiffness at t = 150 ms the velocity fluctuation of the second motor can be distinguished at the (150 < t < 300 ms) because of the abnormality at the mechanical connection and because of the shortage of a second motor velocity observer. Regarding the variation of the second pulley stiffness, the load of the helper motor is immediately decreased, while the corresponding load of the leader motor is increased. This leads to an excess of the torque set point in leader in order to keep up its actual velocity near to the velocity desired. The electromagnetic torque produced in the leader given to the helper as a torque set point. The applied upper value of the torque set point to the helper while having lower load leads to a helper velocity fluctuate which generate a non-damped velocity fluctuation as showed in Fig. 9. In this specific approach, the velocity of helper motor is uncontrollable, and then it is free to fluctuate from point *E* to *D* and vice versa pursuing the leader electromagnetic torque that has been previously mentioned in Fig. 4.

Resembling results are extracted in the state of a steady variation of the pulley stiffness coefficients and particularly by adjusting k_{p2} = 0.6k_{p1} (Fig. 10) During the start-up, a slight velocity fluctuation of the helper motor can be observed which is significantly incremented at higher velocities. The velocity fluctuation of the helper motor becomes much more severe in the steady-state operation. This fluctuation in mechanical system is likely to cause resonance phenomena resulting to torsional vibration, maintenance problems, early component exhaustion and sound pollution problems. By using elastomer-type couplings between the major components is a mechanical method to enable as much damping overall the system. To decrease the menace of such potential problems, an electrical way is to certify an improved connection between the sub-systems by proposing electrical damping in the state of velocity fluctuations at the electromechanical system.

Evaluating Figs. 6 and 7 with Figs. 9 and 10, it should be figured out that, if both leader and helper control by velocity controller, the motors velocity keep equal to its reference value even in the state of a variation at the mechanical connection line while requiring a more value of torque from the other one leading to an unbalanced load sharing. So, in the state of leader velocity controlled and helper torque controlled, the electromagnetic torque of motor can be maintained to a specific desired value. But, the motor velocity varies slightly depending on the load keeping accidentally the electromagnetic torque of motor stable.

In this paper, the conception of a proper and acceptable controller based on the regard of the corresponding velocity and torque mutual errors is proposed that is responsible to balance both electromagnetic torques and motor velocities. This approach should be evaluated as inevitable for a smooth operation having simultaneously the mechanical burden identically shared to the DMDs.

6.3 Combined Velocity–Torque Controller

To solve the clear drawbacks of the aforementioned approaches, a combined control approach is proposed as applicable for DCBLDC motors drive when balance load sharing is required. In this approach, the both motors are concurrently torque and velocity controlled aiming to ensure the same performance at the state of a distinction at the mechanical connection line. The analytical diagram of the proposed approach is shown in Fig. 11. A velocity PI controller handles the first motor velocity error (reference velocity-actual velocity) and generates a corresponding reference signal. Simultaneously, a second torque PI-controller is incorporated in parallel with the velocity PI-controller

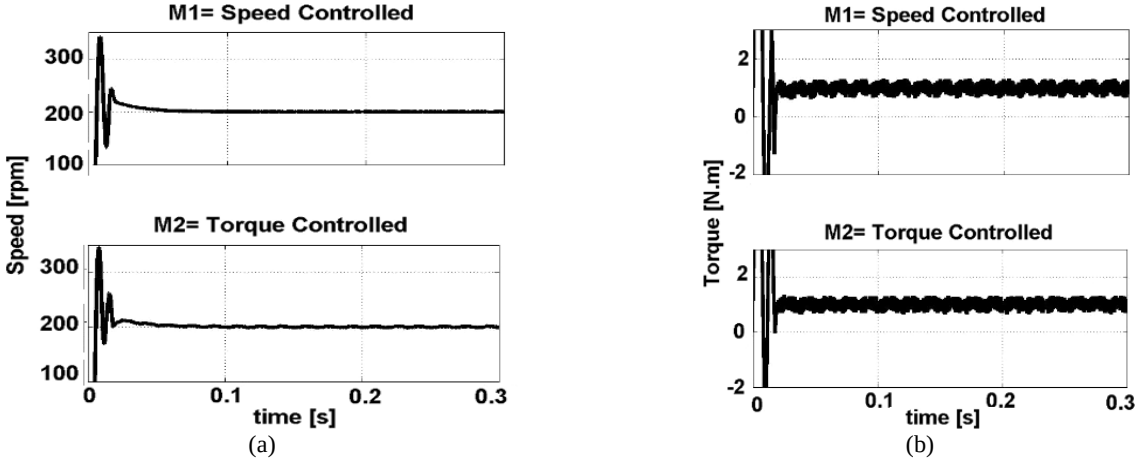

(a) (b)

Fig. 10 Leader–helper motor performance applying a velocity controller at the leader motor and a torque controller at the helper: simulation results with a steady variation at the pulley stiffness coefficients (k_{p2}=0.6k_{p1}).

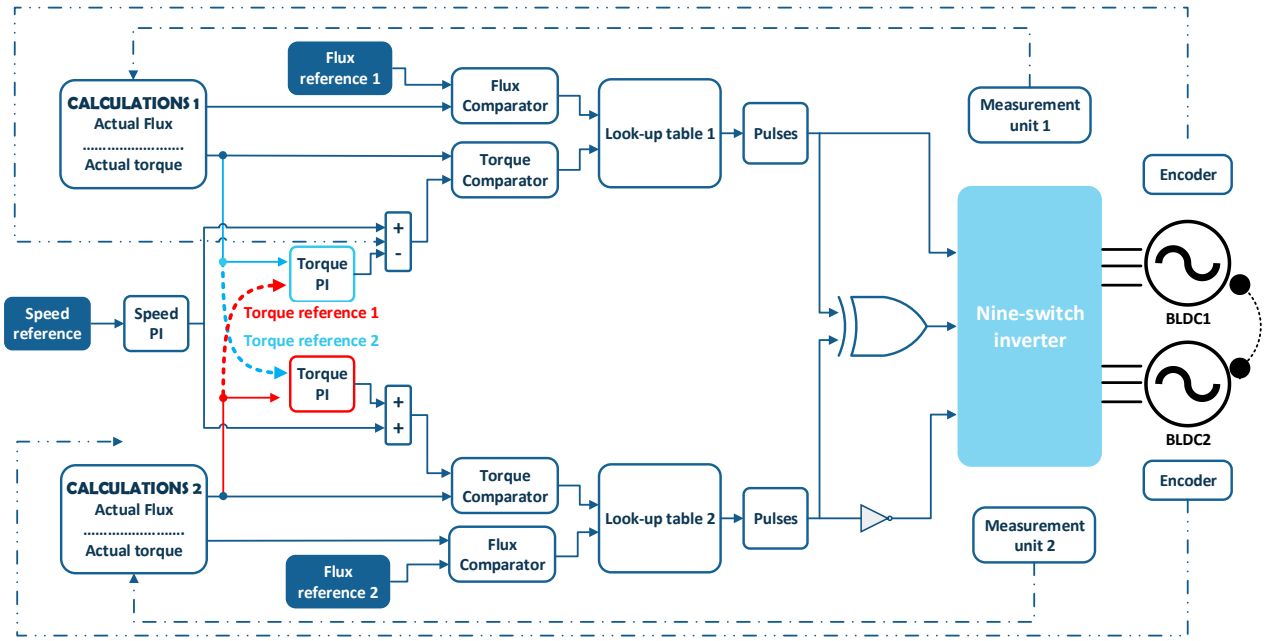

Fig. 11 Detailed diagram of the proposed combined approach of DCBLDC drive operation.

which in turn generates a reference signal using as the division of the amounts of the both motors torques. The output signals of the torque and velocity PI controllers are sum together, and the resultant is used as a set point of torque utilized by the torque comparator. This is important to mentioned that using similar a parallel controller, the two PI-controllers must be carefully set up relative to each other to prevent instabilities. It means that the velocity PI-controller must be faster than the torque PI-controller. The primary step in designing these controller is to firstly apply a fast PI-velocity controller in order to prevent the advent of velocity fluctuations. As the same way, the additional slower PI-torque controller will be responsible to use the electromagnetic torques difference of the two motors aiming to omit the corresponding error. It is necessary to mention that the output signals of the two PI-controllers of the first sub-system are subtracted whereas the same outputs signal of the second sub-system are added. This depends on how the electromagnetic torque error is defined. In the system under study in this paper, the specific torque error handled by the PI-torque controllers has been defined as T_{e1}–T_{e2}.

Using the exclusively proposed approach, the two motors can either be leader or helper in association with the mechanical burden at their shaft, so there is no leader–helper configuration. Hence, this approach could be assumed as equivalent to a mutual compensation of mechanical disturbances between the two drives acting as an “electrical damper”.

The simulations performed in the previous sections in the identical case studies are shown in Figs. 12 and 13 for the proposed approach. The configuration of the velocity PI-controllers was maintained similarly, and the coefficients of the PI-torque controllers used for the simulation were adjust at k_p = 0.2, k_i = 0.2. A small degradation at the velocity of first motor can be considered in Fig. 12 at t = 150 ms. Simultaneously, the second motor velocity is increased a little, whereas the first motor velocity is decreased as a result due to the decrease of the helper mechanical load. However, due to the presence of the velocity controller for the two motors, both motor velocities remains at the reference values. In addition, the total load torque equally divides between two motors and there are no deviations from the reference value.

Comparing the results of the proposed combined approach with the two previously above mentioned control approaches, it should be considered that the motor performance is similar to the state of a dual velocity approach except that the steady torque error emerging at Fig. 6 (dual velocity approach) for t >150 ms has been omitted at Fig.12(a) due to them extra torque controller, which has been appended to the proposed control approach. Similarly, it should be observed that the motor performance is similar to the state of leader velocity controlled-helper torque controlled except that the velocity fluctuation appearing at Fig. 9 (leader velocity controlled-helper torque controlled) for t >150 ms has been omitted at Fig.12(a) due to them additional velocity controller, which has been appended to the proposed control approach. Comparison velocity fluctuations for proposed controller corresponding to leader–helper velocity controller is showed in Fig. 12(b).

In the state of a steady variation of the mechanical connection line, the combined approach is firstly responsible to remain the motors at the identical velocity preventing any motor velocity fluctuation,

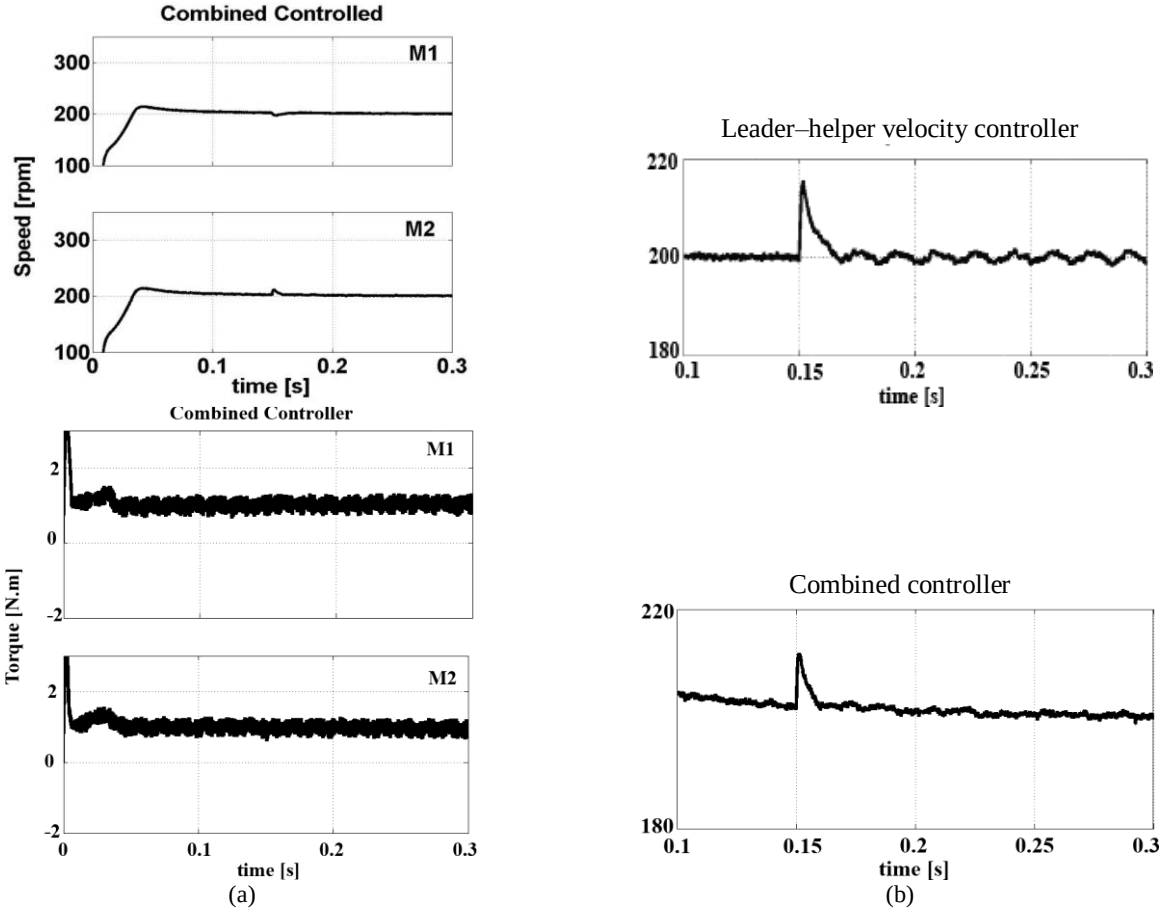

Fig. 12 Dual motors drive performance; a) applying the proposed Combined approach: simulation results with 40% reduction of the helper pulley stiffness coefficient k_{p2} at t = 15 s and b) comparison velocity fluctuations for proposed controller corresponding to leader–helper velocity controller (Fig. 9).

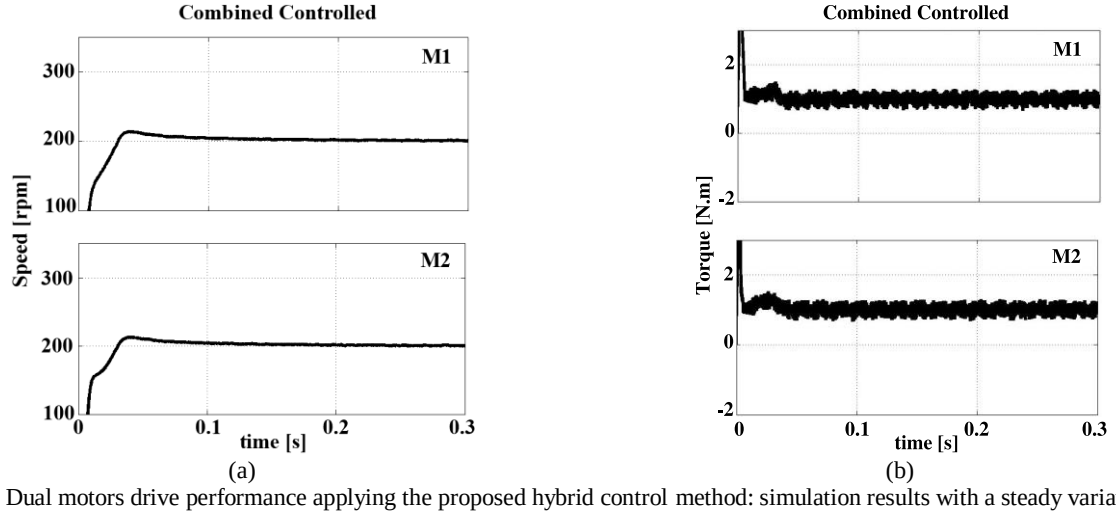

Fig. 13 Dual motors drive performance applying the proposed hybrid control method: simulation results with a steady variation at the pulley stiffness coefficients (k_{p2}=0.6k_{p1}).

while the torque controller uses the corresponding error of electromagnetic torque aiming to balance the mechanical burden between the two BLDC motors. The PI-controller operation under this condition is showed in Fig. 13.

7 Experimental Result

In order to validation the efficiency and the consistency of the proposed approach, an accurate under-scale laboratory DCBLDC drive has been made. The particular drive consists of two BLDC motors and a DC motor as load, three pulleys couplings with a common elastic belt, and an electrical control board. The system rotation is consists of two three phase, four-pole BLDC motors, 120 W each, supply by a NSIs. The use of single inverter supplied by an AC/DC converter

unit is also designed and implemented. A variable velocity-torque drive has been constructed using an improved DTC method for NSI. The current of two phases and the common DC voltage are measured separately for drive using Hall effect transducers. A DSP microprocessor was used DSPIC33FJ256MC710 motor control family to realize the needed IDTC principles. An experimental setup of the drive system is presented in Fig. 14. In order that the difficulty to experimentally model a sudden variation of the pulley stiffness, the performances of the three approaches are studied in the state of a steady variation at the common mechanical connection line caused by a misalignment. So, the leader drive (M2) was intentionally installed with misalignment of approximately 2° in relation to its initial alignment. In the experimental studies, the velocity reference remains to value 200 r/min. To calculate the torque, first the velocity controller is set to the reference value. According to torque and velocity DC motor curves, the torque and current corresponding to this velocity is extracted from the DC motor curves. Finally, with the change of the resistance connected to the motor terminal, the current is adjusted at the calculated value.

7.1 Experimental Results: Leader Velocity Controlled–Helper Velocity Controlled

The experimental results are presented in Fig. 15 to verify the validity of operations of the dual velocity approach at both leader and helper drive (Fig. 5) and centralization on the velocities and motors torques. The electromagnetic torque ripple can be observed caused by the IDTC yet. The experimental results done having the coefficient of the PI-velocity controllers adjust to $k_{p\text{-velocity}} = 5$ and $k_{p\text{-velocity}} = 1$. It can be considered, due to existence of the dual separated velocity control so the both motor velocities are quite the same, the motor torques are different a little, because of unbalance load sharing at the shaft of motors caused by the 2° misalignment. That means that the leader motor undertakes more percentage of the burden result to distribution of unequal load. These experimental results shown at Fig. 7 simulating a dual motor shaft misalignment.

7.2 Experimental Results: Leader Velocity Controlled–Helper Torque Controlled

The system performance using a velocity controller at the leader and a torque controller at the helper (Fig. 8) is presented in Fig. 16. There is a significant velocity fluctuation of the helper motor similar to the velocity fluctuation which is illustrated in Fig. 10, because there is no any velocity PI-controller of the helper, velocity fluctuations are may be observed and also the helper motor pursue the leader motor electromagnetic torque. These ripples experimental drive operation likely lead to expanded vibrations of the overall system. These vibrations had to be cleared quickly to avoid the equipment from irreparable damages. It is analytically and experimentally demonstrated that using this approach in a DMD with an abnormally in mechanical system, there is identical response particularly of the helper in which fluctuations of the motor velocity are occurred demonstrating ripples operation. This can be described considering that, these ripples are depend on the mechanical properties of the system such as moments of inertias, stiffness coefficients, damping coefficients and different dimensions.

7.3 Combined Velocity–Torque Control

In order to elimination the leader motor overloading reported in the aforementioned conventional approaches, the proposed combined approach was implemented having the coefficients of the PI-velocity controllers adjust to $k_{p\text{-velocity}} = 5$, $k_{i\text{-velocity}} = 1$ and the coefficients of the PI-torque controller to $k_{p\text{-torque}} = 0.2$, $k_{i\text{-torque}} = 0.5$. Fig. 17 shows the motor torques and the motor velocities. It is evident that the error of electromagnetic torque at the steady-state duration has been reduced compared with the corresponding performance when the dual separated velocity control is applied. In the state of the combined approach showing that the load is shared between two motors equally and

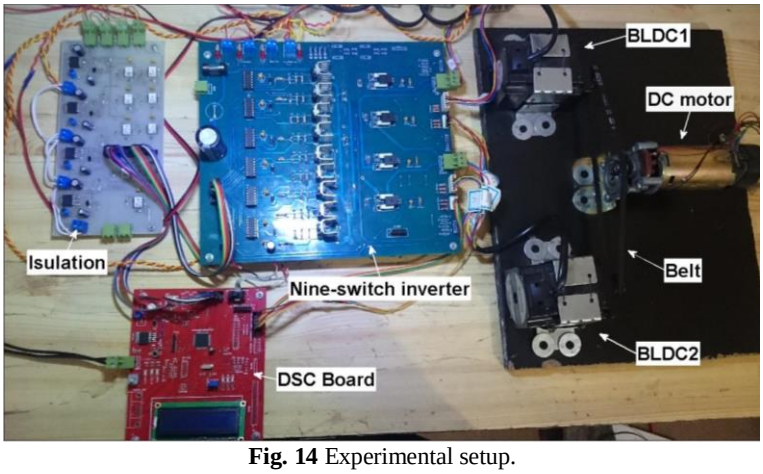

Fig. 14 Experimental setup.

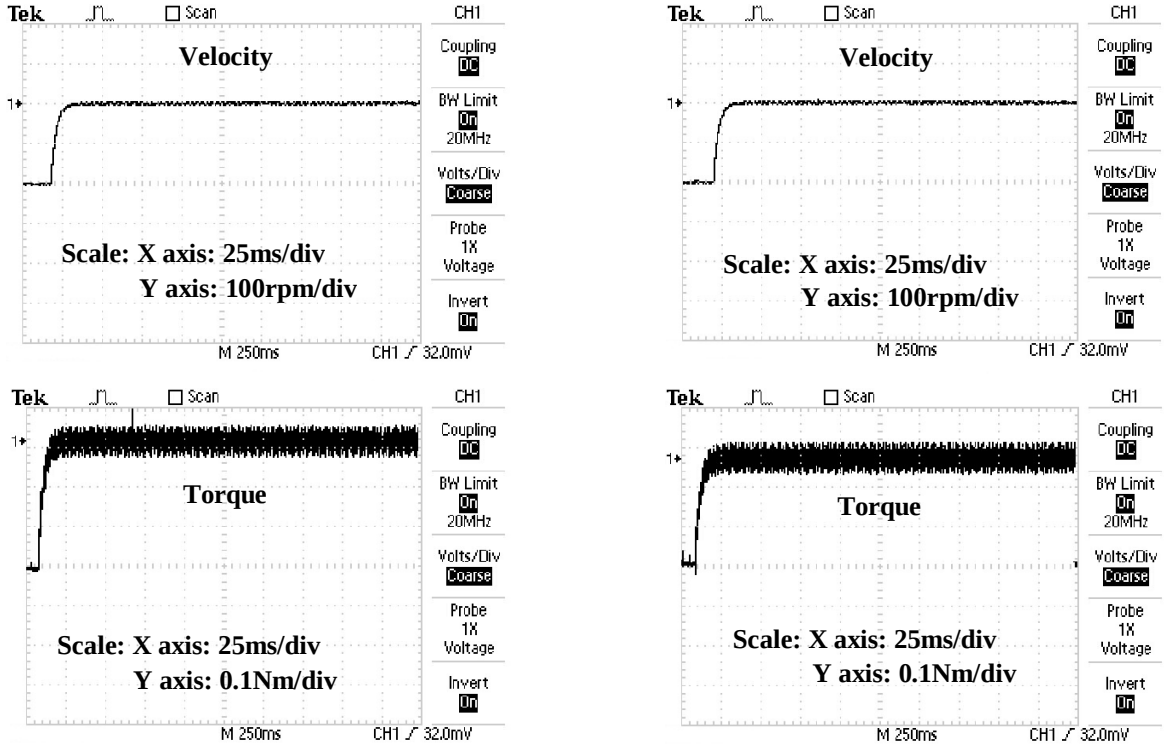

(a) (b)

Fig. 15 Dual velocity controller at both leader and helper motors: experimental results with a steady variation at the second pulley stiffness coefficients caused by misalignment of the leader drive. a) Leader and b) Helper motor.

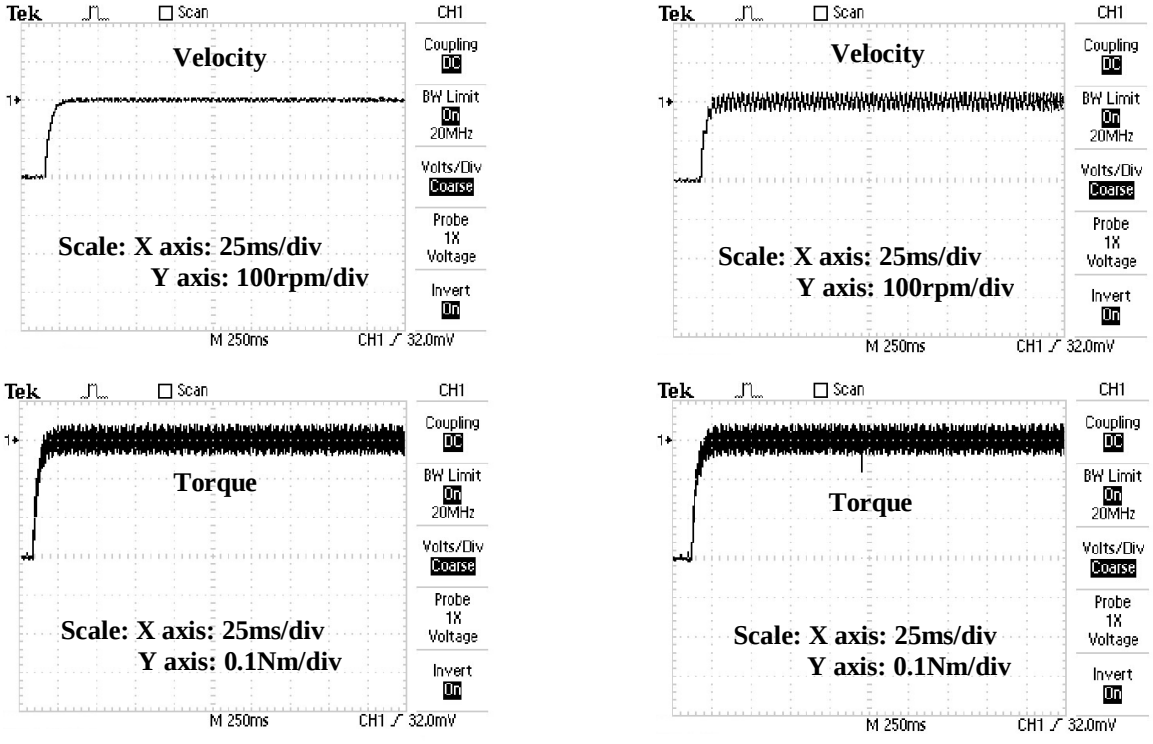

(a) (b)

Fig. 16 Velocity controller at the leader motor and a torque controller at the helper: experimental results with a steady variation at the pulley stiffness coefficients caused by misalignment of the leader drive. a) Leader and b) Helper motor.

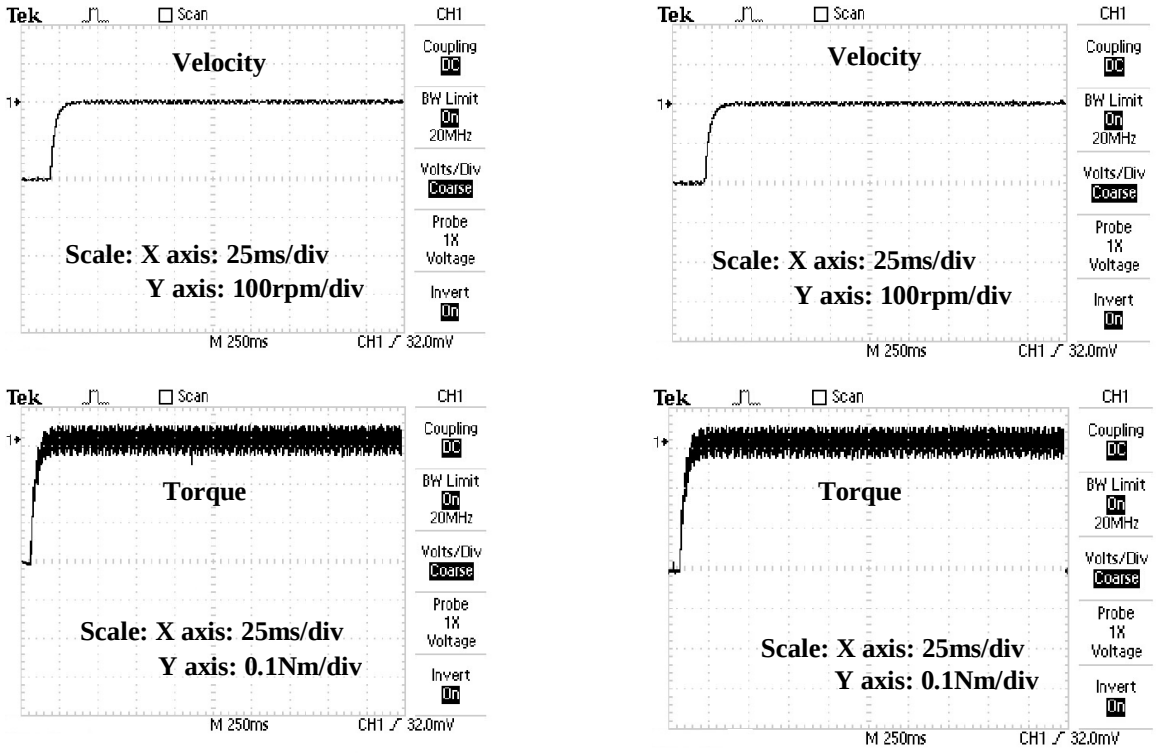

(a) (b)

Fig. 17 Proposed hybrid approach: experimental results with a steady variation at the pulley stiffness coefficients caused by misalignment of the leader drive. a) Leader and b) Helper motor.

they are approximately identical operation point of the characteristic velocity-electromagnetic torque curve. Therefore, the proposed approach is effective and can be successfully applied for minimization of both velocity and torque error.

8 Conclusion

A new combined approach for DMD utilizations with a common mechanical load is being studied in this paper that using IDTC, which is very effective for two coupled motors drive system. The proposed approach is applicable for cases that there is a requirement for power control just through one control board to supply two motors. This method is only able to control the torque and velocity of each motor independently using a single inverter and controller. The combination of two drives in a nine-switch integrated topology has resulted in smaller dimensions and lower costs than the classical two inverter topologies. Using analytical relationships and simulation results, it became clear that the proposed approach has a significant advantage over other methods in controlling two motors, especially when there is an abnormal condition such as the difference in the stiffness coefficient of mechanical connection line. Distribution of balanced load in motors and mitigation of fluctuations by proper setting of controlling velocity and torque coefficients are unique features of the proposed approach and this method has the ability of dealing with potential abnormalities in the mechanical connection line. Simulation results are also experimentally verified using a laboratory system properly constructed to simulate a drive operation. A variation of the mechanical connection line was made by locating one motor with an arbitrary misalignment between to the two motors shaft. The experimental responses evidence that the proposed method surpasses among the other approaches making obvious that it can be trusty applied in a DCBLDC to moderate possible exhaustions at the mechanical connection line.

References

[1] V. Khanna, *Insulated gate bipolar transistor IGBT theory and design*. Wiley-IEEE Press, 2003.

[2] A. H. Almarhoon, Z. Q. Zhu, and P. L. Xu, "Improved pulsating signal injection using zero-sequence carrier voltage for sensorless control of dual three-phase PMSM," *IEEE Transactions on Energy Conversion*, Vol. 32, No. 2, pp. 436–446, 2017.

[3] T. Bernardes, V. Montagner, H. Grundling, and H. Pinheiro, "Discrete time sliding mode observer for sensorless vector control of steady magnet synchronous machine," *IEEE Transactions On Industrial Electronics*, Vol. 61, No. 4, pp. 1679–1691, Apr. 2014.

[4] Y. Jiang; W. Xu, Ch. Mu, and Yi. Liu, "Improved deadbeat predictive current control combined sliding mode strategy for PMSM drive system," *IEEE Transactions on Vehicular Technology*, Vol. 67, No. 1, pp. 251–263, 2018.

[5] M. L. Masmoudi, E. Etien, S. Moreau, and A. Sakout, "Amplification of single mechanical fault signatures using full adaptive PMSM observer," *IEEE Transactions on Industrial Electronics*, Vol. 64, No 1, pp. 615–623, 2017.

[6] K. W. Lee, S. Park, and S. Jeong, "A seamless transition control of sensorless PMSM compressor drives for improving efficiency based on a dual-mode operation," *IEEE Transactions on Power Electronics*, Vol. 30, No. 3, pp. 1446–1456, Dec. 2012.

[7] P. K. Singh, B. Singh, V. Bist, K. Al-Haddad, and Ambrish, "BLDC motor drive based on bridgeless landsman PFC converter with single sensor and reduced stress on power devices," *IEEE Transactions on Industry Applications*, Vol. 54, No. 1, pp. 625–635, 2018.

[8] H. Shin and J. I. Ha, "Phase current reconstructions from DC-link currents in three-phase three-level PWM inverters," *IEEE Transactions on Power Electronics*, Vol. 29, No. 2, pp. 582–593, Feb. 2014.

[9] B. G. Cho, J. I. Ha, and S. K. Sul, "Analysis of the phase current measurement boundary of three shunt sensing PWM inverters and an expansion method," *Journal of Power Electronics*, Vol. 13, No. 2, pp. 232–242, Mar. 2013.

[10] H. Lu, X. Cheng, W. Qu, S. Sheng, Y. Li, and Z. Wang, "A three-phase current reconstruction technique using single DC current sensor based on TSPWM," *IEEE Transacions on Power Electronics*, Vol. 29, No. 3, pp. 1542–1550, Mar. 2014.

[11] P. M. Kelecy and R. D. Lorenz, "Control methodology for single inverter, parallel connected dual induction motor drives for electric vehicles," in *Proceedings of 1994 Power Electronics Specialist Conference-PESC'94*, Vol. 2, pp. 987–991, 1994.

[12] F. Xu, L. Shi, and Y. Li, "The weighted vector control of velocity-irrelevant dual induction motors fed by the single inverter," *IEEE Transacions on Power Electronics*, Vol. 28, no. 12, pp. 5665–5672, Dec. 2013.

[13] I. X. Bogiatzidis, A. N. Safacas, E. D. Mitronikas, and G. A. Christopoulos, "A novel control strategy applicable for a dual AC drive with common mechanical load," *IEEE Transactions on Industry Applications*, Vol. 48, No. 6, pp. 2022–2036, Nov./Dec. 2012.

[14] K. Matsuse, H. Kawai, Y. Kouno, and J. Oikawa, "Characteristics of velocity sensorless vector controlled dual induction motor drive connected in parallel fed by a single inverter," *IEEE Transactions on Industry Applications*, Vol. 40, No. 1, pp. 153–161, Jan./Feb. 2004.

[15] H. I. Dokuyucu and M. Cakmakci, "Concurrent design of energy management and vehicle traction supervisory control algorithms for parallel hybrid electric vehicles," *IEEE Transactions on Vehicular Technology*,Vol. 65, No. 2, Feb. 2016.

[16] D. Bidart, M. Pietrzak-David, P. Maussion, and M. Fadel, "Mono inverter multi-parallel steady magnet synchronous motor: structure and control strategy," *IET Electric Power Applications*, Vol. 5, No. 3, pp. 288–294, 2011.

[17] E. Foch, G. Bisson, P. Manussion, Pietrzak-David, and M. Fadel, "Power system comprising several synchronous machines synchronously self controlled by a converter and control method for such a system," *U.S. Patent 7538501*, Mar. 2007.

[18] N. L. Nguyen, M. Fadel, and A. Llor, "A new approach to predictive torque control with dual parallel PMSM system," in *IEEE International Conference on Industrial Technology (ICIT)*, pp. 1806–1811, Feb. 2013.

[19] J. M. Lazi, Z. Ibrahim, M. H. N. Talib, and R. Mustafa, "Dual motor drives for PMSM using average phase current technique," in *IEEE International Conference on Power and Energy*, pp. 786–790, 2010.

[20] A. Del Pizzo, D. Iannuzzi, and I. Spina, "High performance control technique for unbalanced operations of single-VSI dual-PM brushless motor drives," in *IEEE International Symposium on Industrial Electronics*, pp. 1302–1307, 2010.

[21] Z. Jian, W. Xuhui, and Z. Lili, "Optimal system efficiency operation of dual PMSM motor drive for fuel cell vehicles propulsion," in. *IEEE 6th International Power Electronics and Motion Control Conference*, Wuhan, China, pp. 1889–1892, 2009.

[22] L. Jian, C. Dawoon, and Y. Cho, "Analysis of rotor eccentricity in switched reluctance motor with parallel winding using FEM," *IEEE Transactions on Magnetics*, Vol. 45, No. 6, pp. 2851–2854, 2009.

[23] H. Chen, G. Xie, and J. Jiang, "The two switched reluctance motors parallel drive system," in *Canadian Conference on Electrical and Computer Engineering*, Toronto, Canada, Vol. 1, pp. 569–572, 2001.

[24] M. S. D. Acampa, A. Del Pizzo, D. Iannuzzi, and I. Spina, "Predictive control technique of single inverter dual motor AC brushless drives," in 18th *International Conference on Electrical Machines*, Vilamoura, Portugal, pp. 6.1–6.9, Sep. 2008.

[25] K. H. Low, S. Prabu, and A. P. Pattathil, "Initial prototype design and development of hybrid modular underwater vehicles," in *IEEE International Conference on Robotics and Biomimetics*, Kunming, China, pp. 311–316, Dec. 2006.

[26] M. Yang, C. Wang, D. Xu, W. Zheng, and X. Lang, "Shaft torque limiting control using shaft torque compensator for Two-inertia elastic system with backlash," *IEEE Transactions on Mechatronics*, Vol. 21, No. 6, pp. 2902–2911, May 2016.

[27] S. H. Kia, H. Henao, and G. Capolino, "Torsional vibration effects on induction machine current and torque signatures in gearbox-based electromechanical system," *IEEE Transacions on Indutrial Electronics*, Vol. 56, No. 11, pp. 4689–4699, 2009.

[28] J. H. Kuang and A. D. Lin, "Theoretical aspects of torque responses in spur gearing due to mesh stiffness variation," *Mechanical Systems and Signal Processing*, Vol. 17, No. 2, pp. 255–271, Mar. 2003.

[29] J. Lin and R. G. Parker, "Mesh stiffness variation instabilities in two-stage gear systems," *Journal of Vibration and Acoustics*, Vol. 124, No. 1, pp. 68–76, Jan. 2002.

[30] S. Xu, S. Eben Li, X. Zhang, B. Cheng, and H. Peng, "Fuel-optimal cruising strategy for road vehicles with step-gear mechanical transmission," *IEEE Transacions on Intelligent Transportation Systems*, Vol. 16, No. 6, pp. 3496–3507, Jun. 2015.

[31] C. Liu, B. Wu, N.R. Zargari, D. Xu, and J. R. Wang, "A novel three-phase three-leg AC/AC converter using nine IGBTs," *IEEE Transacion on Power Electronincs*, Vol. 24, No. 5, pp. 1151–1160, 2009.

[32] L. Zhang, P. C. Loh, and F. Gap, "Compact integrated energy systems for distributed generation," *IEEE Transactions on Industrial Electronics*, Vol. 60, No. 4, pp. 1492–1502, 2013.

[33] M. Alizadeh. P, M. Sanatgar, and A. Bali, "Dead-time optimisation with reducing voltage distortion for nine-switch inverter," *International Journal of Electronics*, Vol. 105, No. 3, pp. 426–445, Apr. 2017.

[34] R. Krishnan, *Steady magnet synchronous and brushless DC motor drives*. CRC Press, 2010.

[35] I. Takahashi and T. Noguchi, "A new quick-response and high-efficiency control strategy of an induction motor," *IEEE Transactions on Industry Applications*, Vol. IA-22, No. 5, pp. 820–827, Sep. 1986.

M. Sanatgar was born in Iran 1985. He received the B.Sc. degree in Electrical Engineering from The University of Guilan, Iran, in 2009, M.Sc. degree in Electrical Engineering from The University of Guilan - Iran, in 2012. He is currently working toward the Ph.D. degree in Electrical Machine Drive from The Malek Ashtar University of Technology. His major research interest includes reliable and efficient control of inverters fed coupled brushless motors applied in automotive systems.

M. R. Alizadeh Pahlavani was born in iran in 1974. He received the B.Sc., M.Sc., and Ph.D. degrees in Electrical Engineering from the Iran University of Science and Technology (IUST), Tehran, Iran, in 1998, 2002, and 2009, respectively. He is Associate Professor of Malek Ashtar University of Technology, Tehran, Iran. He is the author of more than 350 journal and conference papers in field of electromagnetic systems, electrical machines, power electronic, FACTS decvices, and pulsed powerr.

A. Bali Lashak is Assistant Professor of Malek Ashtar University of Technology, Tehran, Iran. He is the author of more than 50 journal and conference papers in field of electromagnetic systems, pulsed power.